IET Science, Measurement & Technology

Research Article

IET Journals
The Institution of Engineering and Technology

Design and implementation of dielectric windows for detection of radial deformation of HV transformer winding using radar imaging

ISSN 1751-8822
Received on 2nd September 2018
Revised 1st October 2019
Accepted on 24th December 2019
E-First on 4th March 2020
doi: 10.1049/iet-smt.2018.5485
www.ietdl.org

Masoume Mahmoodi[1] ✉, Seyyed Mahdi N.R. Abadi[1], Hossein Karami[2], Maryam A. Hejazi[3], Gevork B. Gharehpetian[2]

[1]*Computer Science and Engineering School, Australian National University, Acton, Canberra, Australia*
[2]*Electrical Engineering Department, Amirkabir University of Technology, Hafez St., Tehran, Iran*
[3]*Department of Electrical and Computer Engineering, University of Kashan, Kashan, Iran*
✉ *E-mail: masoume.mahmoodi@anu.edu.au*

Abstract: The synthetic aperture radar (SAR) imaging method has been recently proposed for online radial deformation detection of high voltage transformer windings. In this method, electromagnetic waves should be transmitted toward the transformer windings through an antenna. The antenna should be moved along the height of the transformer. Since electromagnetic waves cannot penetrate the metal tank, a window is required on the body of the transformer tank to transmit waves toward the winding. The proper design of such a window and investigation of SAR imaging methods with the existence of it, is necessary to make the previous SAR imaging studies applicable to the transformer winding. Therefore, in order to study the design and implementation of a dielectric window, a prototype of a tank with a dielectric window is built considering electrical and mechanical constraints. The experimental results show the feasibility of applying the SAR imaging for localisation of radial deformation with the existence of a dielectric window in real transformers.

1 Introduction

The power transformer is one of the main elements and expensive parts of power transmission and distribution networks which has a valuable role in interconnecting networks and reducing network losses and voltage drop. Thus, their outage may cause a blackout of the power system and harm the economy [1]. Many faults which lead to the transformer outage are caused by transformer windings deformation. Therefore, transformer windings deformation detection and localisation, especially in the early stages, are very important to extend the lifetime of transformers and reduce the maintenance cost [2, 3].

Several methods have been investigated for online power transformer monitoring. In 2012, the application of synthetic aperture radar (SAR) imaging for transformer monitoring had been introduced [4]. In this method, electromagnetic waves are transmitted by an antenna to the transformer windings and the reflected waves are received by a receiver antenna. In order to form a two-dimensional (2D) image of the transformer winding to obtain further information from transformer windings, like type, location and extent of mechanical defects, transmitter and receiver antennas have been moved alongside the height of the winding and as a result, the object is seen from different angles. The procedure for collecting information is called the SAR imaging method [5]. The results of sound and defected states are stored in a database and a coloured image of each state is generated. The images are compared and if there is any difference in them, it means that defection occurs. In [6–8], this method has been extended and the defect location has been detected. However, the existence of the transformer tank, which is a conductor and does not let the waves pass through it, has not been considered.

In [9], the necessity of installing a window on the transformer tank, which enables the waves to pass through the tank, has been noted. The window should be made of an insulating material, which passes waves with minimum losses and reflections. The merits of insulation windows are ease of implementation on the transformer tank, no interference with the performance of insulating parts of the transformer, possibility of installation and removal of sensors while the transformer is working and, the most important one, allowing online monitoring of partial discharge (PD) using electromagnetic-based methods, studied in recent years. In some cases, the insulation window has been used to detect PD [10–13].

In [13], a dielectric window has been constructed to install an ultra-high frequency (UHF) sensor on one side of the single-phase 18 MVA power transformer tank for detecting PD. In this dielectric window, an electrical insulating material, which is compatible with oil, has been installed on the window. In [12–14], in order to install an antenna for the detection of PD, the window has been made of epoxy resin or polytetrafluoroethylene (PTFE) insulators. In [15], a dielectric window has been designed to prevent oil leakage, create a shield against the electrical field at power frequency, and provides the possibility for UHF waves to exit through the transformer and received using the antenna mounted behind the transformer. However, none of the mentioned windows has the capability of use in SAR imaging method.

The dielectric windows should provide the possibility of installing the antenna on the transformer without any need to take the transformer out of service. These windows make the possibility of monitoring several transformers using only one set of devices. In other words, the antennas and the monitoring system can be mounted on a transformer and after scanning that transformer, it can be unmounted to be used on another transformer, while the transformers are in service. In addition, it should be ensured that the antennas do not measure external noise by insulating them from the external environment. In all the aforementioned papers, dielectric windows are designed to detect PD, while for mechanical defects detection of transformer windings using the SAR imaging method, they cannot be useful because the antennas should be moved alongside the tank. In the rest of the paper, the transformer windings only refer to HV transformer winding.

In this paper, dielectric windows are designed for a single-phase transformer tank to make detection of radial deformation of HV transformer winding using the SAR imaging method applicable. The design of these windows is important because their application leads to online monitoring of mechanical defect, and so, it will improve the useful lifetime of transformers and reduce maintenance costs. It should be noted that these windows, not only can make the implementation of the SAR imaging method for

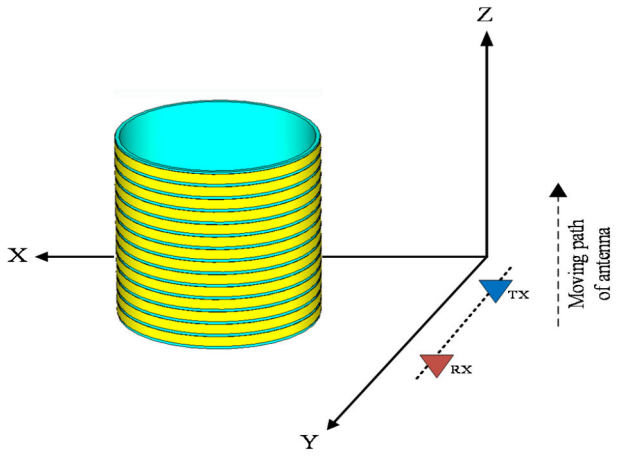

Fig. 1 *Imaging method-scheme [18]*

mechanical defect detection of transformer windings possible, but also can be used as a dielectric window for PD detection, which is not the main purpose of this paper. The designed windows should be impermeable to oil, withstand maximum reservoir temperature, do not disfigure the integrity of the tank, have sufficient mechanical strength to endure stress within the tank and must be capable of tolerating the maximum pressure inside the tank caused by oil (which is 0.8 bar for most transformers). The study of mechanical constraints is carried out using ABAQUS software. Then a prototype of a single-phase tank with dielectric windows is constructed and its ability to provide the possibility of radial winding deformation detection using the SAR imaging method is shown through tests conducted on an actual winding in the presence of this tank and windows. In addition, the practicability of the proposed design is discussed for three-phase transformers and a scheme for three-phase transformer tanks equipped with dielectric windows is presented. The main contributions of the paper are summarised as follows:

- Select epoxy glass as the dielectric in the designed window that enables electromagnetic waves penetration and has sufficient mechanical and thermal strengths.
- Studying electrical, mechanical and thermal constraints of the dielectric window for the real transformer condition.
- Design a transformer tank equipped with dielectric windows for the online monitoring of HV windings.
- Investigation of applicability of the SAR imaging method in the existence of a dielectric window in a real transformer winding.

The rest of the paper is organised as follows: In Section 2, the radar imaging is briefly explained. In Section 3, appropriate material is selected based on tests for installation in a dielectric window. In Section 4, suitable locations for dielectric windows are determined and the proposed design is presented for a single-phase transformer tank with dielectric windows. In Section 5, the validation of the proposed design is carried out through experimental tests and the results are presented. In Section 6, the practicability of the design is evaluated for three-phase transformers and finally, Section 7 concludes the paper.

2 SAR imaging method

One of the most up-to-date methods for the diagnosis of radial deformation of the transformer's winding is the SAR imaging method, which is still under study and improvement. In Fig. 1, the imaging process is shown. A Gaussian pulse is sent by the transmitter antenna, and the signal is propagated into the environment. When the wave hits the target, a part of its energy is reflected and received by the receiver antenna. The received signal provides 1D information about the transformer. Additional information to create a 2D image from the winding can be provided by changing the position of the antennas and repeating the process of sending and receiving pulses in different positions alongside the height of the transformer [4, 16, 17].

The transmitted signal has several paths in its routes from the transmitter antenna to the target (winding) and from target to the receiver antenna. These paths are due to reflections from the walls and the floor of the surroundings. These paths create undesired components in the received signal. In order to delete these defective data, desired time delay of the signal should be calculated for the shortest and longest paths between the antennas and the target, so, the received signal should be considered in the time duration of t as $T_{\min} \le t \le T_{\max}$, where $T_{\min}$ and $T_{\max}$ are the shortest and longest time delays, respectively [18].

In order to convert the received signals into a 2D image, the Kirchhoff migration algorithm is used in this paper. Detailed descriptions of how to create a 2D image from the transformer have been expressed in [4]. The final formulation of the Kirchhoff migration method to plot a 2D image for this problem is as follows:

$$\Psi(id_0, jd_0) = \sum_{k=1}^{K} \frac{d_M \cdot jd_0}{2\pi \cdot R^2 \cdot v \cdot T_s} \times \sum_{k} [f(kd_M, (n+1)T_s) - f(kd_M, nT_s)]|_{nT_s = 2(R/v)} \quad (1)$$

where i and j are the number of pixels on the X and Z axes, respectively. K is the number of measurement points and k is the kth measuring point. d_0 is the minimum mesh size in the X–Z plane, d_M is the distance between two measuring points, kd_M is the place of the antenna on the X-axis, v is the wave velocity, T_s is the sampling time, $f(.)$ is the value of the field in the boundary and R is the distance between the antenna and observation point.

According to (1), at each point in the X–Z plane $\Psi(x_i,z_j)$ presents the wave reflection coefficient at that position, which is between 0 and 1 [5]. Each value can be presented by colour. Using the colour definition, the target image is generated by plotting the absolute value of $\Psi(x_i,z_j)$. Cold and hot colours express medium and high reflections from the transformer windings, respectively. A shorter distance between the transformer and the antennas leads to higher reflection. If the image of a winding has more/less warm colours, compared with its previous image obtained at installation time, it can be said that there is a convex/concave radial deformation in it. This approach is known as an image correlation method in the literature [18]. By analysing multiple images obtained from the SAR imaging method, the number 0.45 is considered as the threshold of warm colours. Since the same number is used as the threshold for both sound and defected winding images, the same conclusion can be obtained with different threshold values as will be discussed further in Section 5.2.

3 Material

The first step in designing a dielectric window is to determine an appropriate dielectric material for installation in this window. This

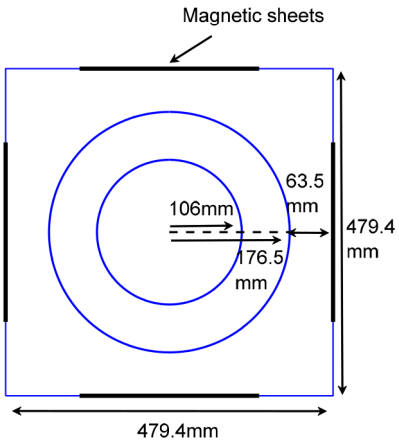

Fig. 2 *Dimensions of the windings and tank of the three-phase transformer 125 MVA and 66/230 kV*

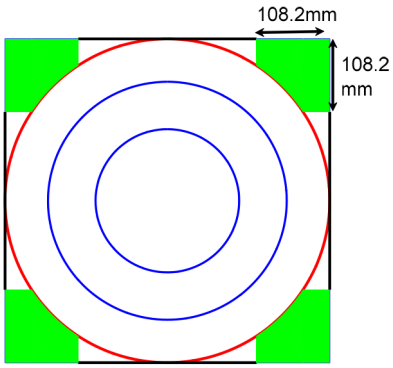

Fig. 3 *Limitations for installing dielectric windows. Green areas, red circle and bold black lines show the suitable locations for the dielectric windows, clearance distances of the windings and electromagnetic sheets, respectively*

material should be able to transmit electromagnetic waves with low losses and reflections, and have good mechanical and thermal strengths. PTFE and epoxy resin are suitable insulators for long-term use in transformers [10]. In [12–14], PTFE has been used as a dielectric in the structure of a window to detect PD, because of its chemical properties and moisture impermeability. In addition, composite materials such as epoxy glass are used in some rectifier transformers and converters to reduce losses of eddy currents because of their high current in the low voltage side [19].

The material used in a dielectric window must have sufficient mechanical strength to withstand the pressure of 0.8 bar, the temperature of 100°C and the imposed mechanical stresses. Some of the important characteristics of the proposed materials are given in Table 1. According to Table 1, epoxy glass has higher mechanical strength than PTFE and seems to be more suitable.

4 Dielectric window placement

4.1 Suitable locations for dielectric windows

The suitable locations for installing the dielectric windows are determined by studying the structure of single-phase transformers. The studies reveal that limitations are the electromagnetic sheets placed in front of each winding, clearance distances of the windings and considerations of antennas such as far-field restriction. As an example, the dimensions of single-phase 1600 kVA transformer are shown in Fig. 2 [20]. According to the map, there is a series of steel sheets in front of the HV winding, which is known as the electromagnetic sheets. These sheets are insulated and compressed together mounted in front of the winding on the body of the tank. Therefore, due to the presence of these sheets, the windows cannot be installed in front of the winding. In addition, the clearance distances of the winding are shown in Fig. 3 by red lines indicate that the antennas cannot be placed at these intervals.

Table 1 Important characteristics of PTFE and epoxy glass

Property	Unit	PTFE	Epoxy glass
tensile strength	MPa	26.9	300
compressive strength	MPa	24.13	180
flexural strength	MPa	do not break	340
dielectric constant	—	2.1	5.5
tanδ	—	0.0002	0.04

Table 2 Specification of the PulseON 220 as the transceiver

Characteristics	Value
pulse repetition frequency	9.6 MHz
centre frequency	4.7 GHz
time interval between scans	20 ms
bandwidth	3.2 GHz

Table 3 Specifications of 1600 kVA windings

Characteristics	Value
rated power	1600 kVA
winding's height	536 mm
HV winding	external diameter: 353 mm
	internal diameter: 237 mm
LV winding	external diameter: 212 mm
	internal diameter: 186 mm

One of the most suitable antennas for broadband applications, especially for UWB applications, is a Vivaldi antenna. In this study, the antenna has a length, width, and thickness of 9.2, 7.6 and 0.0508 cm, respectively, and the bandwidth of 3–10 GHz. However, since the transceiver hardware, PulsON 220 [5], has the frequency range of 3.1–6.3 GHz, the antennas are used in the range of PulseON. The specifications of the PulsON 220, as the transceiver device, are given in Table 2. In order to maximise the output radiated power, the antenna should be pointed to the target on its maximum gain and it requires the target to be located at the far-field region of the antenna to reduce its effects on antenna radiation pattern [21], given by the following inequality:

$$r \geq 2\frac{D^2}{\lambda} \tag{2}$$

where D is the longest antenna length, λ is the wavelength, and r is the distance between the antenna and the target. In this study, D is 9.2 cm. Therefore, according to Table 2 and (2), the minimum distance between the antenna and the winding should be 35 cm. With consideration of the location of the sheets, the clearance distance of the winding and the considerations related to the Vivaldi antenna, places where dielectric windows can be installed are shown in Fig. 3 with a green colour for the 1600 kVA transformer.

4.2 Proposed design

According to Table 3, the clearance distance of the understudy winding is ~63.5 mm. Considering the three limitations described in Section 4, suitable locations to install the dielectric windows are the corners of the tank, as shown in Fig. 4. According to the minimum distance between the antenna and the winding, which is 35 cm, and the winding's radius, which is 17.65 cm, the minimum size of the tank and dielectric windows are determined and shown in Fig. 4.

The 3D view of the tank is shown in Fig. 5 by considering the dielectric windows. To install the epoxy glass on the body of the tank, two internal and external flanges are used for each window. The internal flange is placed on the metal body of the tank. After mounting the epoxy glass on this flange, it is tightened on the body of the tank using the external flange.

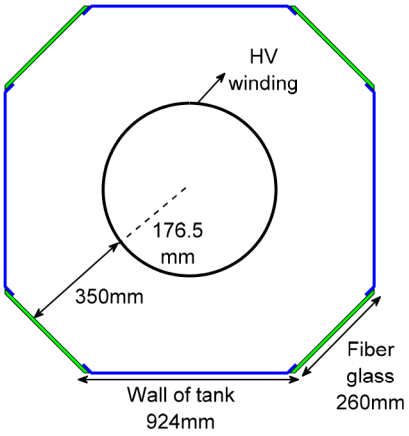

Fig. 4 *Proposed design of a single-phase transformer tank*

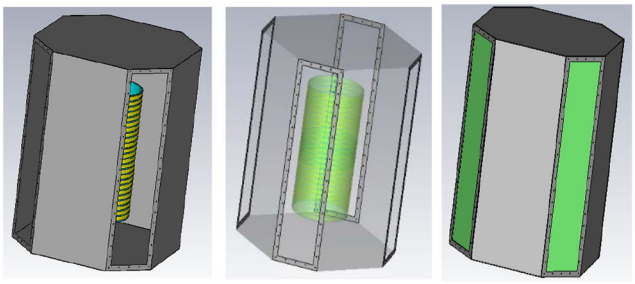

Fig. 5 *3D view of the single-phase transformer tank with dielectric windows*

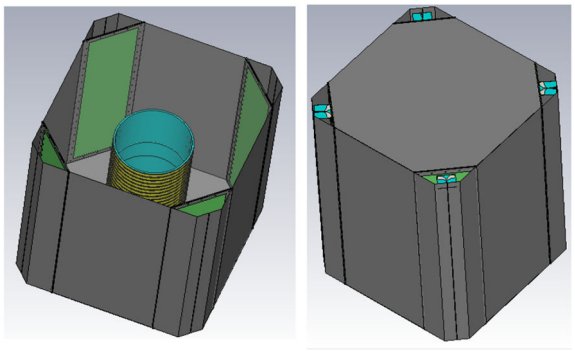

Fig. 6 *3D view of the proposed design of a single-phase transformer tank equipped with four dielectric windows and the antennas in the corners*

Power transformers are installed in substations that are affected by various magnetic fields and noises from surroundings. To prevent the negative effects of these magnetic fields on the installed antennas, a metal enclosure can be used behind antennas as shown in Fig. 6.

After designing the tank and before its fabrication, the mechanical analysis of the proposed design using the ABAQUS software is required to ensure that the proposed design is practicable from a mechanical point of view. As shown in Fig. 7*a*, only one-quarter of the tank is modelled, because the proposed scheme for the tank is symmetric. In this simulation, a washer is used to seal the window. The displacement of the entire set, the stress contours for the metal tank and the epoxy glass sheet are shown in Figs. 7*b–d*, respectively. According to the numerical results, maximum stress on the tank and glass epoxy sheet is much less than the yield strength of their materials and in fact, there are no plastic deformations on the entire set, so it is not necessary to assess low cycle fatigue for these parts. As well as this, the entire set is subjected to static loading, therefore high cycle fatigue is not considered as a damage mechanism for them. As a consequence, it could be asserted that the tank and glass epoxy sheets are in safe conditions quietly. Moreover, the simulations are under critical conditions of a transformer at the temperature of 100°C and a pressure of 0.8 bar, while in the actual conditions temperature and pressure are less than these amounts, and as a result, the displacement and stresses on the tank are less in the actual condition.

5 Results of experimental studies

5.1 Experimental setup

In order to monitor one side of the winding, two antennas, one in the transmitter mode and the other one in the receiver mode, are required. The presence of two windows is sufficient to detect the defect of one side of the winding, and if the defect is on the other side of the winding, it will be detected by two other antennas. The dimensions of the designed tank are shown in Fig. 8. The height of the tank is related to the winding height and in the designed tank, it is considered 550 mm.

The antennas are moved along a vertical imaging path. A lifting system is used for moving the antennas in this direction, as indicated in Fig. 9. The path is divided into 27 measuring points. The distance between two consecutive points is considered to be 2 cm. At each point, 100 scans are transmitted and recorded. Measured data is given to the Kirchhoff migration algorithm after several processing steps, including the deletion of defective data as described in Section 2, selection of suitable time window and averaging as described in [4]. The Kirchhoff migration algorithm maps the data of different points that are a function of time and location (x,t) to the $\Psi(x,z)$ function. By drawing this function, the

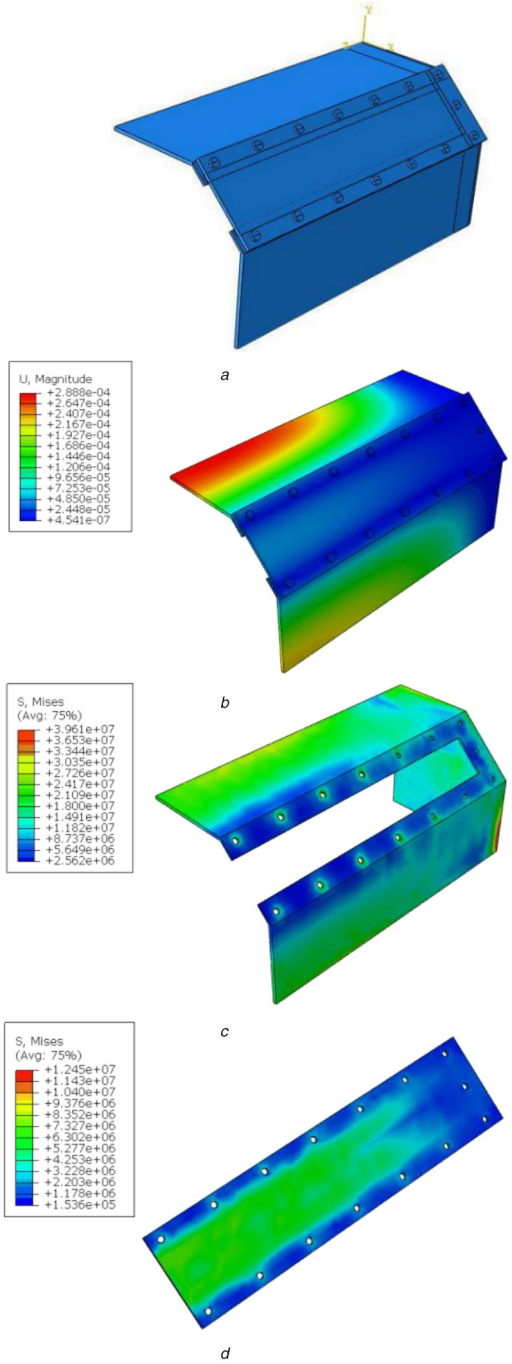

Fig. 7 *ABAQUS simulation results for mechanical analysis of the proposed tank design*
(a) Model of a quarter of the tank, ***(b)*** Displacement of the entire set, ***(c)*** Stress contours for the metal tank, ***(d)*** Stress contours for epoxy glass sheet

2D image of the transformer is obtained. Fig. 9 shows the setup of an experimental study, where the imaging route in front of the transformer winding is vertical. It shows that in this case, the path of the antennas is along the Z-axis.

In order to model the radial deformation, a laboratory model of this deformation is used. The artificial deformation on the winding is similar to the previous studies [4, 5]. The height of this deformation is 6 cm, which covers about four disks of the winding, as shown in Fig. 9*b*. The width and length of the deformation are 4 and 5.2 cm, respectively.

5.2 Radar imaging results without tank

First, it is necessary to get the image of the sound transformer as the reference image. This image is depicted in Fig. 10. In addition, Fig. 11 illustrates the image of the winding in the presence of radial deformation in the lower part of the winding. The images of the winding when the radial deformation is in middle and upper parts have not been included due to the lack of space.

In order to determine that the location of the radial deformation is in upper, middle, or lower parts of the winding, the stored data from the SAR imaging process is used to find the number of warm colours in each part. For example, the data of the sound winding obtained from the scanning process at 27 points, is divided into three 9-point parts, for the upper, middle and lower parts. Even though for each part, the antennas are imaging the whole or most of the winding, the spatial/angular resolution is higher for the scanned part in comparison with the other two parts. In other words, the sensitivity of the images is higher for the part which is being scanned in each step. This division method is carried out for sound and defected images. The results of applying this method on the images are listed in Table 4. As can be seen in Table 4, the difference between the sound and defected Table 4, the difference between the sound and defected images are more distinguishable and obvious with a value of 0.45 as the threshold. There is no difference in the procedure for different windings. The important part of the proposed procedure is that the condition of the sound

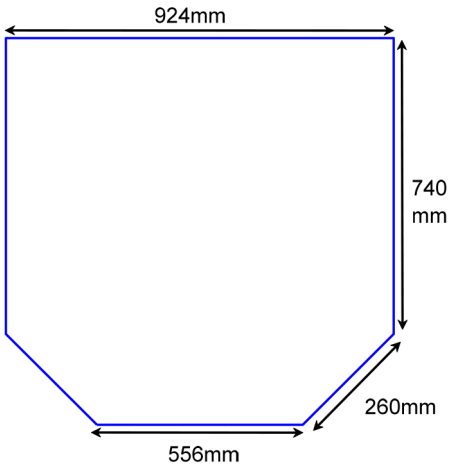

Fig. 8 *Dimensions of the constructed single-phase transformer tank used in the experiments*

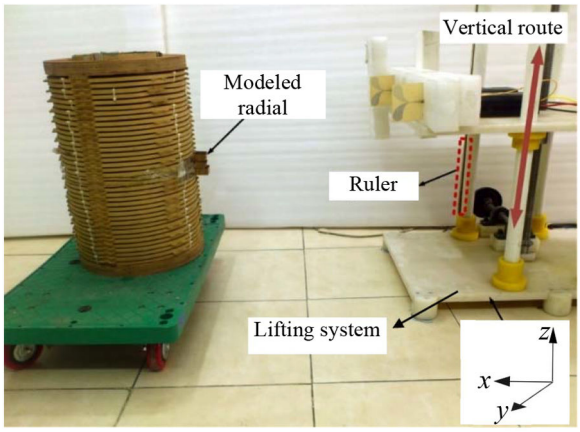

a

b

Fig. 9 *Test set up*
(a) Vertical test set up neglecting the tank, ***(b)*** Dimensions of the artificial deformation on the winding

and deformed states are the same except in the deformed part of winding and we must use the same threshold for comparison of warm colours in sound and deformed states. In other words, if we use 0.45 for determining the number of warm colours in the sound state, this number should be used in the future for determining the number of warm colours to detect the deformed state. These results show the efficiency of the image processing method in the detection of radial deformation. In this method, useful information can be obtained about deformation in all segments of the transformer because vertical imaging data is divided into lower, middle and upper parts. For example, if the radial deformation is in the middle part of the winding, the comparative parameter has a higher value in the middle part which means that the radial deformation is in this part [9]. The same discussion can be drawn for radial deformation in the lower and upper parts. Localisation of the defect can be more accurate by creating the images of the winding in the smaller divisions which is not the aim of this paper.

5.3 Radar imaging results in the presence of a tank and the dielectric window

The test setup in the presence of the tank is shown in Fig. 12. In this setup, antennas are located at a distance of 45 cm from each other, in front of each dielectric window and in the corner of the tank. The radar imaging process is the same as before in this case. Fig. 13 shows the sound winding image in this setup. Comparing

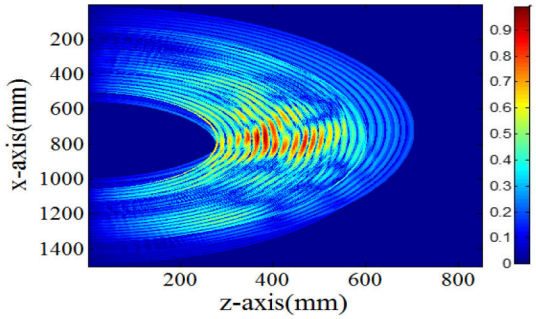

Fig. 10 *Image of the sound transformer as a comparison reference, neglecting the tank*

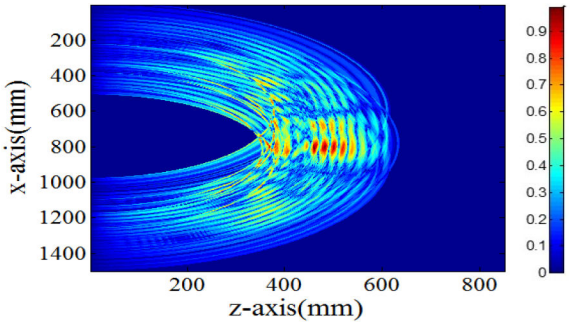

Fig. 11 *Image in the presence of radial deformation neglecting the tank in the lower part of the winding*

Table 4 Radar imaging results for radial deformation neglecting the tank, with different thresholds

Location of radial deformation	Part of the image	Number of coloured points for different thresholds		
		0.3	0.45	0.5
upper part	upper	173,654	159,644	155,988
	middle	158,006	138,766	136,444
	lower	162,727	142,543	137,234
middle part	upper	160,233	145,506	142,007
	middle	183,652	177,543	171,666
	lower	167,928	139,786	138,038
lower part	upper	168,332	147,132	144,099
	middle	165,604	142,560	140,954
	lower	180,591	163,152	159,978

Fig. 12 *Vertical test set up considering the tank*

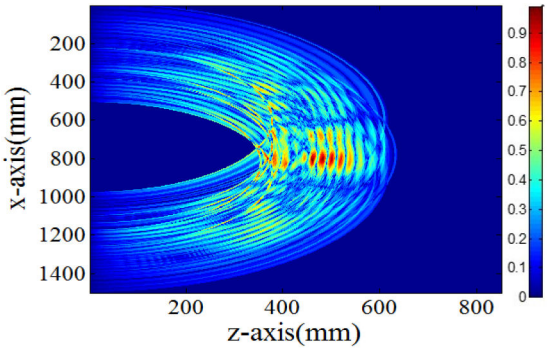

Fig. 13 *Image of the sound transformer as a comparison reference considering the tank*

this image with Fig. 11 shows that the presence of the tank causes an increase in blue curves and general confusion in the image. Then, radar imaging is carried out in the same setup but with the modelled deformation at the top, middle and bottom of the winding. The result of this test, when the deformation is in the lower part is shown in Fig. 14. Table 5 indicates that the part which includes the deformation has more warm colours. The results in this section verify that the radar imaging technique is capable of

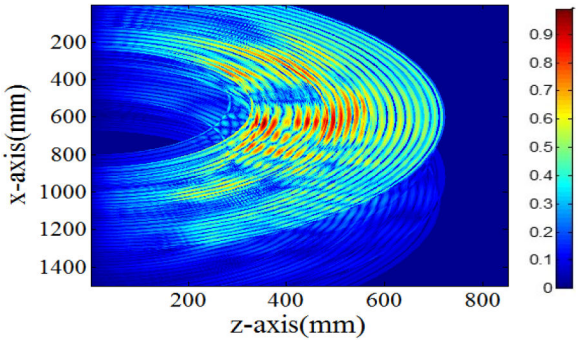

Fig. 14 *Image in the presence of radial deformation considering the tank in the lower part of the winding*

recognising, the radial deformation in the transformer windings considering the presence of the tank.

6 Practicability on three-phase transformers

Since most of the transformers used in the actual power networks are three-phase transformers, the capability of the proposed design should be evaluated for them. Considering the three limitations explained in Section 4, which are the location of the electromagnetic sheets, the clearance distance of the windings, and the considerations related to the Vivaldi antenna, suitable places of the dielectric windows are shown in Fig. 15 in green colour. The grey lines show the monitored area of the windings by the Vivaldi antenna. As shown in this figure, in order to monitor one side of each winding, two Vivaldi antennas are required. Hence, eight Vivaldi antennas are needed to monitor all three windings of a transformer. In another approach, two antennas can be used to monitor each side one after another. Fig. 16 shows the proposed final design for three-phase transformer tanks to monitor windings by electromagnetic waves. In order to prevent the adverse effect of external magnetic fields on the antennas, a metal enclosure is placed behind each antenna to insulate the antenna against external magnetic fields and noises. The metal enclosure should be covered by electromagnetic absorbers to prevent the reflection of the wave from this.

Table 5 Radar imaging results for radial deformation considering the tank

Location of radial deformation	Number of points with coloured number greater than 0.45
upper part	upper part of the image: 80,163
	middle part of the image: 35,077
	lower part of the image: 44,279
middle part	upper part of the image: 38,026
	middle part of the image: 43,566
	lower part of the image: 40,185
lower part	upper part of the image: 41,134
	middle part of the image: 39,497
	lower part of the image: 70,026

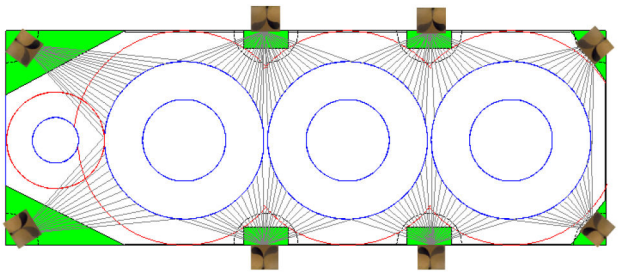

Fig. 15 *Coverage of all three windings of the transformer with 8 Vivaldi antennas*

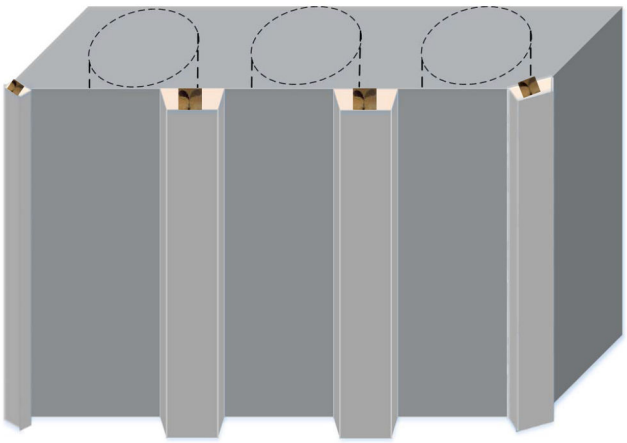

Fig. 16 *Design of the proposed three-phased tank with metal enclosure behind the antennas to insulate the antennas against external magnetic fields and noises*

7 Conclusion

In this paper, single and three-phase transformer tanks, which are equipped with dielectric windows, have been investigated. In the first step, a suitable material for the dielectric window has been selected to let the waves pass through with minimum losses, and good mechanical and thermal strength. In the next step, the suitable sizes and locations for installing dielectric windows have been determined according to the transformers' limitations, which are the electromagnetic sheets placed in front of the windings, clearance distances of the windings and considerations of the antennas such as far-field restriction. The mechanical analysis has been carried out by ABAQUS software and the mechanical strength of the designed tank has been verified through simulations. Based on these studies, a prototype of the designed tank has been built. Then, the radar imaging has been used to detect the radial deformations with and without the tank. The results show the effectiveness of the application of the proposed window in determining the approximate location of the radial deformation using the SAR imaging method. It should be emphasised that the implementation of this window makes it feasible to apply the SAR imaging on the transformer winding. A further extension would be to implement the proposed, designed dielectric window on an actual in-service distribution transformer to investigate its efficacy.

8 References

[1] Patel, D., Chothani, N.G., Mistry, K.D., *et al.*: 'Design and development of fault classification algorithm based on relevance vector machine for power transformer', *IET Electr. Power Appl.*, 2018, **12**, (4), pp. 557–565

[2] Mahvi, M., Behjat, V.: 'Localising low-level short-circuit faults on the windings of power transformers based on low-frequency response measurement of the transformer windings', *IET Electr. Power Appl.*, 2015, **9**, (8), pp. 533–539

[3] Shintemirov, A., Tang, W.H., Wu, Q.H.: 'Transformer winding condition assessment using frequency response analysis and evidential reasoning', *IET Electr. Power Appl.*, 2010, **4**, (3), pp. 198–212

[4] Golsorkhi, M.S., Hejazi, M.S.A., Gharepetian, G.B., *et al.*: 'A feasibility study on application of radar imaging for detection of transformer winding radial deformation', *IEEE Trans. Power Deliv.*, 2012, **27**, (4), pp. 2113–2121

[5] Ulander, L.M.H., Hellsten, H., Stenstorm, G.: 'Synthetic-aperture radar processing using fast factorized back-projection', *IEEE Trans. Aerosp. Electron. Syst.*, 2003, **39**, (3), pp. 760–776

[6] Mortazavian, S., Shabestary, M., Mohamed, Y.A., *et al.*: 'Experimental studies on monitoring and metering of radial deformations on transformer HV winding using image processing methods and UWB transceivers', *IEEE Trans. Ind. Inf.*, 2015, **11**, (6), pp. 1334–1345

[7] Mosayebi, R., Sheikhzadeh, H., Golsorkhi, M.S., *et al.*: 'Detection of winding radial deformation in power transformers by confocal microwave imaging', *Electr. Power Compon. Syst.*, 2014, **42**, (6), pp. 605–611

[8] Mortazavian, S., Gharehpetian, G.B., Hejazi, M.S.A., *et al.*: 'A simultaneous method for detection of radial deformation and axial displacement in transformer winding using UWB SAR imaging'. 4th Conf. on Thermal Power Plants (Gas, Combined Cycle, and Steam), Tehran, Iran, 18–19 December 2012

[9] Hejazi, M.S.A., Ebrahimi, J., Gharehpetian, G.B., *et al.*: 'Application of ultra-wideband sensors for on-line monitoring of transformer winding radial deformations–a feasibility study', *IEEE Sens. J.*, 2012, **12**, (6), pp. 1649–1659

[10] Judd, M.D., Yang, L., Hunter, I.B.B.: 'Partial discharge monitoring of power transformers using UHF sensors. Part I: sensors and signal interpretation', *IEEE Electr. Insul. Mag.*, 2005, **21**, (2), 5–14

[11] Sufei, L., Yue, H., Haifeng, Y., *et al.*: 'Finite element simulation based sensitivity analysis of UHF sensing modes for PD detection'. Condition Monitoring and Diagnosis (CMD), Bali, Indonesia, 23–27 September 2012

[12] Judd, M.D., Farish, O., Pearson, J.S., *et al.*: 'Dielectric windows for UHF partial discharge detection', *IEEE Trans. Dielectr. Electr. Insul.*, 2001, **8**, (6), pp. 953–958

[13] Judd, M.D., Yang, L., Bennoch, C.J., *et al.*: 'UHF diagnostic monitoring techniques for power transformers'. EPRI Substation Equipment Diagnostics Conf. XII, New Orleans, 15–18 February 2004

[14] Coenen, S.: '*Measurement of partial discharges in power transformers using electromagnetic signals*' (University of Stuttgart, Germany, 2012)

[15] Judd, M.D., Yang, L., Hunter, I.B.B.: 'Partial discharge monitoring for power transformer using UHF sensors. Part 2: field experience', *IEEE Electr. Insul. Mag.*, 2005, **21**, (3), pp. 5–12

[16] Bi, D., Xie, Y., Ma, L., *et al.*: 'Multifrequency compressed sensing for 2-D near-field synthetic aperture radar image reconstruction', *IEEE Trans. Instrum. Meas.*, 2017, **66**, (4), pp. 777–791

[17] Case, J.T., Ghasr, M.T., Zoughi, R.: 'Optimum two-dimensional uniform spatial sampling for microwave SAR-based NDE imaging systems', *IEEE Trans. Instrum. Meas.*, 2011, **60**, (12), pp. 3806–3815

[18] Karami, H., Gharehpetian, G.B., Norouzi, Y., *et al.*: 'GLRT-Based Mitigation of partial discharge effect on detection of radial deformation of transformer HV winding using SAR imaging method', *IEEE Sens. J.*, 2016, **16**, (19), pp. 7234–7241

[19] Raychem, R. P. G.: 'World of specialty transformers'. Available at http://raychemrpg.com/transformers/pdf/catalog-for-transformers.pdf

[20] Irantransfo, C.: '*Design details of 125 KVA power transformer*' (Irantransfo Co., Zanjan, Iran, 2016)

[21] Balanis, C.A.: '*Antenna theory analysis and design*' (John Wiley & Sons, USA, 2012)